

# Conversion of the luminescence of laser dyes in opal matrices to stimulated emission

O.K. Alimov, T.T. Basiev, Yu.V. Orlovskii, V.V. Osiko, M.I. Samoilovich

**Abstract.** The luminescence and laser characteristics of a synthetic opal matrix filled with organic dyes are studied upon excitation by nanosecond laser pulses. The appearance of stimulated emission in a partially ordered scattering medium is investigated. It is shown that if the luminescence spectrum of a dye (oxazine-17) is located far outside the photonic bandgap of the opal matrix, stimulated emission along a preferential direction in the (111) plane is observed when pumping exceeds a threshold even without an external optical cavity. The stimulated emission spectrum is considerably narrower than the luminescence spectrum and consists of several narrow lines located within the dye luminescence band. If the luminescence spectrum of a dye (rhodamine 6G) overlaps with the photonic bandgap of the opal matrix, a different picture is observed. The loss of radiation in the matrix leads to the red shift of the luminescence spectrum, while the stimulated emission as in the case of oxazine-17 lies is observed within the luminescence band.

**Keywords:** photonic crystal, opal, photonic bandgap, luminescence, oxazine-17 and rhodamine 6G dyes, stimulated emission.

## 1. Introduction

The search for new materials (in particular, hybrid materials consisting of porous inorganic matrices with organic impurities) characterised by new types of interactions between the active medium and a matrix is a topical problem. Special attention is paid to nanostructured materials, including a new type of artificial materials with spatially periodic optical characteristics, so-called photonic crystals [1, 2]. It seems that the most promising technologies of producing such media are based on the use of self-organising systems, for example, three-dimensional structures with a regular cubic packing of silicon dioxide (SiO<sub>2</sub>) nanospheres, i.e., opal matrices [3, 4].

Opal matrices consist of many SiO<sub>2</sub> nanospheres of approximately identical diameters, which are packed, as a rule, into a dense face-centered cubic lattice. The regular packing of SiO<sub>2</sub> nanospheres forms a three-dimensional diffraction grating with a period lying in the optical range corresponding to an optical or photonic crystal.

Variations in the production technology of opals result in different degrees of packing of nanospheres and in different degrees of closure of pores. Depending on these characteristics, opal matrices can be divided into two groups: single-domain opal matrices, in which a large volume of the sample has a regular structure (it is these opal matrices that have the properties of photonic crystals) and polydomain opal matrices, containing many regions with regularly arranged nanospheres, which are differently oriented with respect to each other (such matrices can be considered as strongly scattering media).

In this study, spherical SiO<sub>2</sub> particles were obtained by hydrolysis of tetraethoxysilane Si(OC<sub>2</sub>H<sub>5</sub>)<sub>4</sub> in ethanol with ammonia as a catalyst [5]. The hydrolysis leads to the formation of small branched polymer silicon dioxide particles, which were transformed due to the inner polycondensation into amorphous spherical microparticles with an average diameter of 230–280 nm. The sedimentation of the suspension caused by the gravitational force results in the formation of a regular packing of SiO<sub>2</sub> nanospheres on the vessel bottom. After precipitation and removal of the hydrolysate, the ordered precipitate represents a hydrogel with 50%–60 wt % of liquid, which was then annealed to evaporate the liquid and to harden the sample. An electronic-microscope image of the synthesised opal matrix within one domain is shown in Fig. 1.

By filling the voids between spheres in the opal matrices with different optically active materials (possessing, for example, amplifying, nonlinear, or sensor properties), one can form nanocomposites with new, sometimes unique, properties. These properties arise due to a considerable increase in the inner surface of nanocomposites and multiple scattering of light in such structures, as well as due to modification of spontaneous emission conditions when the size of inhomogeneities in the medium is comparable to or smaller than the optical radiation wavelength (Anderson localisation and Purcell effect) [6]. In addition, selective spectral bands for radiation propagation are formed in photonic crystals [1, 2], which leads to changes in the interaction of radiation with matter, including changes in the probabilities of radiative transitions, in the emission spectrum, and in its spatial and polarisation characteristics. The idea of using photonic crystals for creation of lasers

T.T. Basiev, Yu.V. Orlovskii, V.V. Osiko Laser Materials and Technology Research Center, A.M. Prokhorov General Physics Institute, Russian Academy of Sciences, ul. Vavilova 38, 119991 Moscow, Russia; e-mail: orlovski@lst.gpi.ru;

M.I. Samoilovich Tekhnomash Central Research Technological Institute, ul. I. Franko 4, 121108 Moscow, Russia;

O.K. Alimov Institute for Nuclear Physics, Academy of Sciences of Uzbekistan, Ulugbek, 702132 Tashkent, Uzbekistan

Received 23 October 2007

Kvantovaya Elektronika 38 (7) 665–669 (2008)

Translated by M.N. Basieva

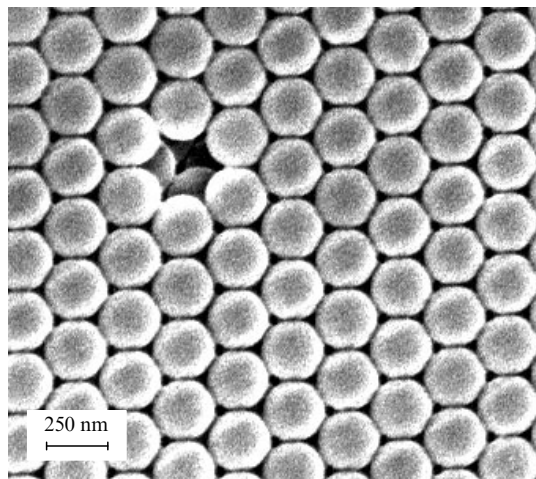


**Figure 1.** Electronic-microscope image of an opal matrix within one domain.

without the threshold was proposed at the early stages of their study [1, 7]. At present, different variants of the development of stimulated emission sources based on photonic crystals are considered [8], namely, lasing due to the optical feedback related to the Bragg reflection in the photonic bandgap, lasing with distributed feedback in a periodic structure, and laser action in a strongly scattering medium.

Lasing without a cavity in an amplifying scattering medium was proposed by Letokhov in 1967 [9] and was achieved for the first time in powders of crystals doped with rare-earth ions [10]. In recent years, stimulated radiation was obtained in dye solutions containing strongly scattering  $\text{TiO}_2$  particles, in  $\text{ZnO}$  powders, and in various polymer matrices filled with dyes. Such radiation is characteristic for systems with a high density of scattering centers, when the mean photon scattering length slightly exceeds the radiation wavelength. If the density of scattering centres is sufficiently high, the emitted radiation may return to the scatterer from which it has been scattered and, thereby forming closed loops. Lasing appears if amplification along individual loops, which work as laser cavities, exceeds losses in them. The lasing frequencies are determined from the condition that the phase shift along the loop should be multiple of  $2\pi$ . The stimulated emission spectrum of such sources contains narrow discrete peaks.

Opal matrices (including matrices with a weakly pronounced polydomain structure) are promising objects for investigation of such processes. The initial polydomain opal matrix is an efficient diffuse scatterer with the mean photon scattering length of  $\sim 8 \mu\text{m}$  for a wavelength of 630 nm (measured using coherent backscattering [11]). A weak opalescence in air is a result of the Bragg diffraction from different crystallographic planes. If such a system is doped with an active medium with a gain sufficiently high to compensate for the losses at least for one of the modes, the scattering medium emits laser radiation. Due to the unusual feedback mechanism, such lasers have some properties that are of interest from both fundamental and practical viewpoints. The authors of [8, 12, 13] demonstrated the possibility of lasing in such systems.

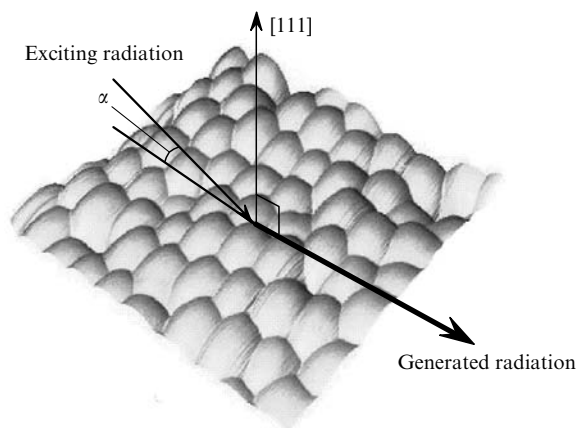
In this work, we study the luminescence and laser characteristics of a synthetic polydomain opal matrix

filled with ethanol solutions of oxazine-17 and rhodamine 6G laser dyes.

## 2. Experimental results

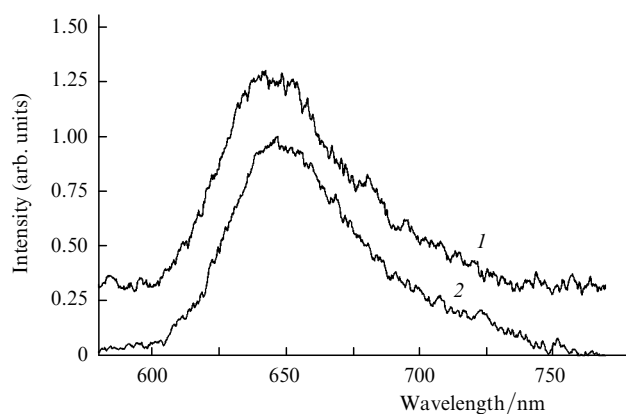
Oxazine-17 was dissolved in ethanol to the concentration  $c = 10^{-3} \text{ M}$  and the solution was poured into a 5-mm thick quartz cell, in which an opal matrix was preliminarily placed. The photonic bandgap measured from the transmission spectrum was located in the wavelength region from 520 to 580 nm and had a maximum at 550–560 nm [for the diameter of  $\text{SiO}_2$  nanospheres of  $\sim 250 \text{ nm}$ ,  $n_{\text{eff}} = 1.37$ , and the angle of incidence of the light beam on the (111) plane close to  $90^\circ$ ]. Measurements were performed after complete filling of the opal pores with the dye solution, and the cell was positioned to avoid spurious reflections.

The geometry of laser excitation and recording of the emission of the opal matrix filled with the oxazine-17 solution is shown in Fig. 2. The opal matrix with oxazine-17 was excited by the 15-ns, 531-nm second harmonic pulses from a Nd:GGG laser at a pulse repetition rate of 12.5 Hz at an angle of  $\alpha$  to the (111) plane, which was varied during experiments. The laser radiation was focused by a lens with the focal length  $F = 80 \text{ mm}$  on the opal matrix surface (spot diameter  $d \sim 500 \mu\text{m}$ ), and the dye emission was projected with a condenser on the slit of a monochromator. The luminescence spectra in the region from 600 to 750 nm were recorded with an MDR-2 monochromator equipped with a FEU-79 photomultiplier operating in the current mode. The luminescence spectra were recorded with the help of a PAR 162/164 Boxcar, which provided the measurement and averaging of instantaneous luminescence signals within a time window  $\Delta t$  at different delay times  $t_d$  with respect to the excitation pulse.



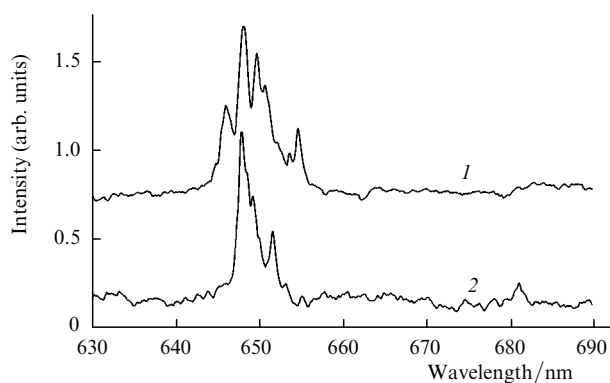
**Figure 2.** Geometry of excitation and recording of stimulated emission of oxazine-17 in opal.

Figure 3 shows the luminescence spectra of the oxazine-17 solution in ethanol and of the same solution introduced to the pores of the opal matrix (hereafter, the delay time is  $t_d \leq 0.5 \text{ ns}$  and the strobe duration is  $\Delta t = 50 \text{ ns}$ ). Luminescence was excited and recorded at the same angles  $\alpha = 45^\circ$  to the sample surface. The luminescence spectra lie in the wavelength region from 600 to 750 nm with the maxima near 650 nm and, at low excitation intensities represent a broad band typical of oxazine-17 in ethanol.



**Figure 3.** Luminescence spectra of the oxazine-17 solution in ethanol (1) and of the same solution in the opal matrix (2)

The luminescence band of the oxazine-17 solution does not overlap with the bandgap of the opal matrix. As the pump intensity increased to  $0.7 \text{ MW cm}^{-2}$  [for a constant angle of  $45^\circ$  between the pump direction and the (111) plane of the opal matrix], the luminescence intensity increases without a change in the spectral profile. The decrease in the pump angle to  $20^\circ$  leads to a significant narrowing of the luminescence spectrum and to the appearance of narrow lines [Fig. 4, curve (1)], the emission in this case propagating along the (111) plane. At the angle  $\alpha = 15^\circ$ , a narrow radiation pattern is preserved and the spectrum narrows even stronger [Fig. 4, curve (2)]. At small angles  $\alpha$ , directional radiation was also preserved in the absence of the quartz cell. It seems that the passage from luminescence to stimulated emission with decreasing angle  $\alpha$  occurs due to an increase in the excited volume of the sample. Thus, we can say that stimulated emission appears in a partially ordered scattering medium.



**Figure 4.** Spectra of directional radiation of the oxazine-17 solution in the opal matrix at  $\alpha = 20^\circ$  (1) and  $15^\circ$  (2).

In subsequent experiments with rhodamine 6G, the exciting laser beam was focused on the sample perpendicular to the (111) plane by using a cylindrical lens providing the maximum excitation volume. Rhodamine 6G was dissolved in ethanol and the solution was poured into a quartz cell. An opal matrix of size  $h = 5 \text{ mm}$  was placed into the cell so that a third of its height was immersed into the solution and two thirds were outside the cell (Fig. 5), which eliminated spurious reflections. Because of ethanol evaporation, the

dye solution in the cell was replaced after each experiment to provide the required concentration of the solution.

Figure 5 shows the position of the opal matrix in the cell and the geometry of excitation and recording of the sample emission. We measured the transmission and luminescence spectra of the rhodamine 6G solution and this solution in the opal matrix in a wide concentration range from  $c = 1.2 \times 10^{-5}$  to  $1.4 \times 10^{-3} \text{ M}$ . Figure 6a presents the transmission spectra of the opal matrix in ethanol, the rhodamine 6G dye solution at  $c = 1.2 \times 10^{-5} \text{ M}$ , and of this solution in the opal matrix. The transmission spectrum of opal in ethanol has a bandgap with the FWHM  $\Delta\nu = 507 \text{ cm}^{-1}$  and the maximum at  $\nu_{\text{max}} = 18050 \text{ cm}^{-1}$ . Filling of the opal matrix with rhodamine 6G does not shift the opal bandgap, which indicates that refractive indices of ethanol ( $n = 1.37$ ) and of the dye solution in ethanol are close to each other.

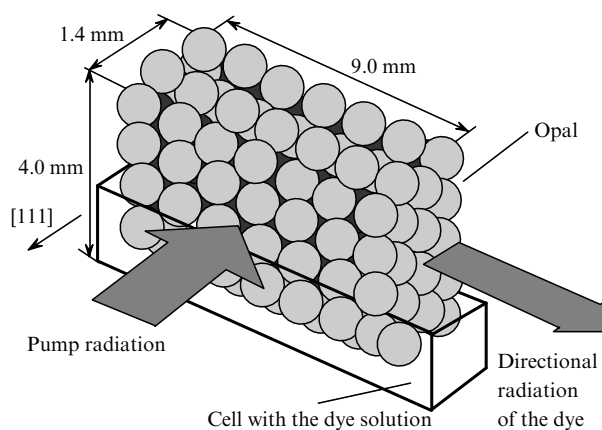


**Figure 5.** Geometry of excitation and recording of stimulated emission of rhodamine 6G in opal.

The luminescence spectra of the rhodamine 6G dye solution were measured in the spectral region  $\nu = 20000 - 15000 \text{ cm}^{-1}$  for the dye solution concentrations  $c = 3.5 \times 10^{-4} - 1.4 \times 10^{-3} \text{ M}$  by the method described above (Figs 6b, c). Luminescence was excited by the 337-nm, 2-ns pulses from a nitrogen laser with a pulse repetition rate of 25 Hz and recorded with an MDR-23 monochromator equipped with a FEU-79 photomultiplier operating in the current regime. As the dye concentration was increased, the maximum of the luminescence spectrum shifted from  $\nu_{\text{max}} = 17984 \text{ cm}^{-1}$  at  $3.5 \times 10^{-4} \text{ M}$  by  $\Delta\nu \leq 365 \text{ cm}^{-1}$  to the red. Further studies of the luminescence properties of rhodamine 6G in opal were performed for concentrations  $c = 3.5 \times 10^{-4}$  and  $1.4 \times 10^{-3} \text{ M}$ . The concentration  $c = 3.5 \times 10^{-4} \text{ M}$  was used because in this case the luminescence band falls into the bandgap of the opal matrix (the luminescence band maximum is shifted from the bandgap center by only  $70 \text{ cm}^{-1}$ ).

Figures 6b, c show the effect of the opal matrix on the luminescence spectrum of rhodamine 6G, which is manifested in the red shift of the luminescence band by  $\Delta\nu = 190 \text{ cm}^{-1}$  with respect to the dye luminescence maximum. The maximum of the luminescence band of the rhodamine 6G solution at  $17619 \text{ cm}^{-1}$  (Fig. 6c) at the concentration  $c = 1.4 \times 10^{-3} \text{ M}$  lies at the long-wavelength wing of the bandgap of the opal matrix and is shifted to the red by

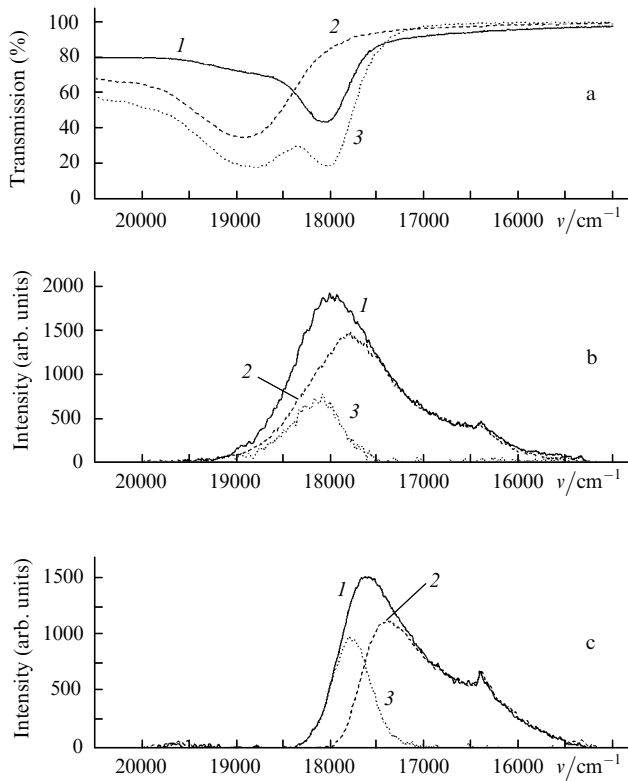


**Figure 6.** Transmission spectra of opal in ethanol (1), of the rhodamine 6G solution ( $1.2 \times 10^{-5}$  M) (2), and of the same solution in opal (3) (a). Luminescence spectra of rhodamine 6G (1) and rhodamine 6G in opal (2) and the difference between these spectra (3) for  $c = 3.5 \times 10^{-4}$  (b) and  $1.4 \times 10^{-3}$  M (c).

$\Delta\nu = 210 \text{ cm}^{-1}$ , when the solution fills the opal matrix. To evaluate the influence of the opal bandgap on the dye luminescence spectra, the luminescence spectra of the dye in opal and ethanol were normalised at the long-wavelength wing, where the bandgap effect is minimal. Curve (3) in Figs 6b, c is the difference between these luminescence spectra. The ratio of the areas under the difference spectrum and under the luminescence spectrum of rhodamine 6G characterises the loss of luminescence inside opal, which is caused mainly by the Bragg reflection.

We obtained stimulated emission in a sample of opal filled with the rhodamine 6G solution without an external optical cavity. The dye-filled opal matrix was excited by the 15-ns, 532-nm second harmonic pulses from a Nd:YAG laser at a pulse repetition rate of 12.5 Hz perpendicular to the (111) plane of the opal matrix (Fig. 5). The pump beam was focused by a cylindrical lens ( $F = 80$  mm) to a strip of size  $0.5 \times 9$  mm and the generated radiation was recorded along the (111) plane of the matrix (at an angle of  $90^\circ$  with respect to the pump beam direction) and projected on the monochromator slit with the help of an optical fiber. We obtained lasing of rhodamine 6G in the opal matrix for three dye concentrations,  $c = 3.5 \times 10^{-4}$ ,  $7.0 \times 10^{-4}$ , and  $1.4 \times 10^{-3}$  M.

The transmission spectra of opal, rhodamine 6G solution, and rhodamine 6G solution in opal pores are shown in Fig. 7a. Figures 7b–d demonstrate the lasing spectra of the ethanol solution of rhodamine 6G in opal and the luminescence spectra of rhodamine 6G in opal at three concentrations excited at 337 nm. One can see that the wavelength  $\lambda_{\text{max}}$  of the maximum of the lasing spectrum of

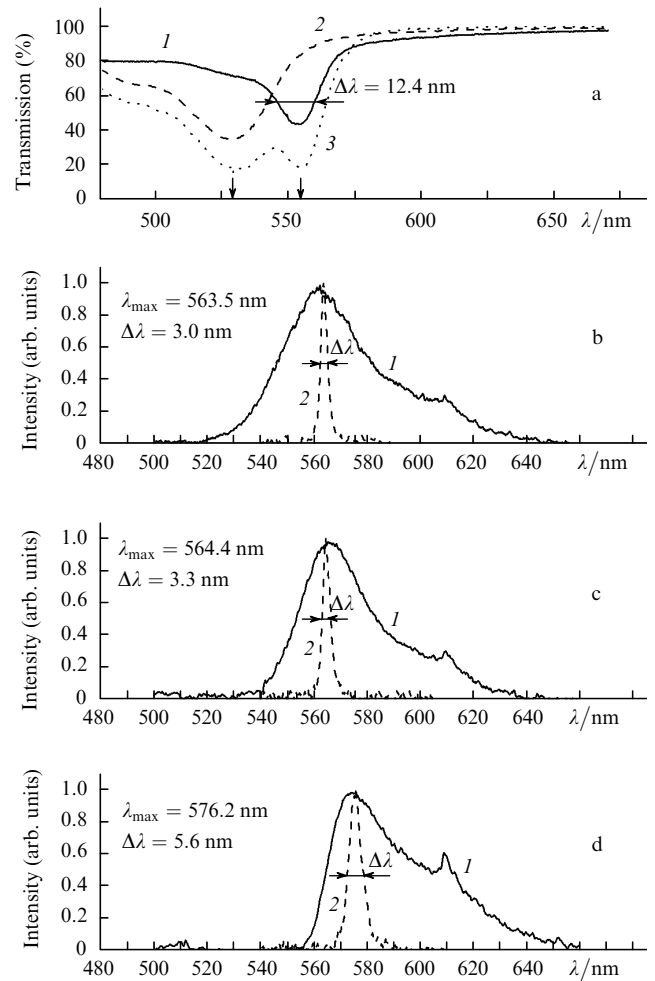


**Figure 7.** Transmission spectra of opal in ethanol (1), of the rhodamine 6G solution (2), and of the same solution in opal (3) (a). Luminescence spectra (excited at 337 nm) of rhodamine 6G (1) and stimulated emission spectra (pumped at 532 nm) of rhodamine 6G in opal (2) for  $c = 3.5 \times 10^{-4}$  (b),  $7.0 \times 10^{-4}$  (c), and  $1.4 \times 10^{-3}$  M (d). The arrows show the pump wavelength (532 nm) and the position of the bandgap maximum (554 nm).

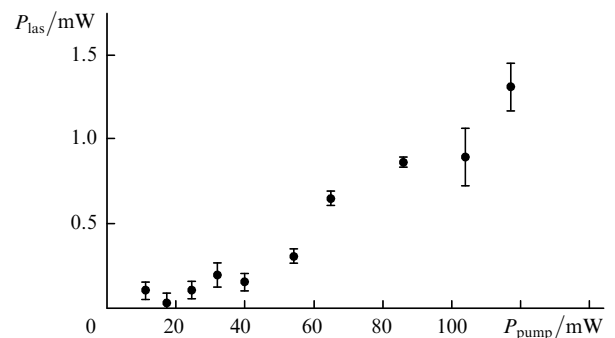


**Figure 8.** Dependence of the radiation power  $P_{\text{las}}$  of the rhodamine 6G solution in ethanol ( $c = 7.0 \times 10^{-4}$  M) in the opal matrix on the pump power  $P_{\text{pump}}$ .

rhodamine 6G in opal approximately coincides with the maximum of its luminescence spectrum in opal and shifts to the red by  $\Delta\lambda = 12.7 \text{ nm}$  with increasing the dye concentration from  $3.5 \times 10^{-4}$  to  $1.4 \times 10^{-3}$  M. Thus, due to the loss in opal, the luminescence maximum shifts to the red, while lasing occurs at a wavelength close to this maximum.

For the dye concentration of  $c = 7.0 \times 10^{-4}$  M, we obtained a linear dependence of the radiation power of rhodamine 6G in opal on the pump power with a threshold pump power of 20 mW and a slope efficiency of 1.2% (Fig. 8). At an average pump power of 120 mW (peak pump power of  $\sim 0.5$  GW cm<sup>-2</sup>), the surface of the opal matrix was destroyed.

### 3. Conclusions

We have obtained stimulated emission in a partially ordered scattering medium on the example of an opal matrix filled with a dye solution. If the luminescence spectrum of the dye lies far from the photonic bandgap of the opal matrix and the power density of nanosecond laser excitation is low, the luminescence of the dye injected into pores of the opal matrix is determined by the spontaneous emission mechanisms and has a broad spectral band coinciding with the spectrum of the dye. Above a pump threshold in the absence of an external cavity, the isotropic radiation transforms into radiation directed along the (111) axis of the opal matrix. The spectrum of such radiation is significantly narrower than the luminescence spectrum and consists of several narrow lines lying within the dye luminescence band. If the luminescence spectrum overlaps with the bandgap of the opal matrix, the maximum of the luminescence spectrum shifts to the red due to the optical loss in the opal matrix caused mainly by the Bragg reflection, and, similar to the previous case, lasing occurs within the luminescence band.

**Acknowledgements.** This work was partially supported by Program No. 8P of the Presidium of the Russian Academy of Sciences, by the Ministry of Education and Science of the Russian Federation according to Contract No. 260/07 with the St. Petersburg State University within the State Contract No. 02 513 11 3186 of 2 May 2007, and by the Russian Foundation for Basic Research (Grant No. 08-02-90040).

### References

1. Yablonoich E. *Phys. Rev. Lett.*, **58**, 2059 (1987).
2. John S. *Phys. Rev. Lett.*, **58**, 2486 (1987).
3. Lopez C. *Advan. Mater.*, **15**, 1679 (2003).
4. Samoilovich M.I., Klesheva S.M., Belyanin A.F., et al. *Microsistem Tekh.*, (6), 3 (2004); (7), 2 (2004); (8), 9 (2004).
5. Stöber W., Fink A., Bohn E. *J. Colloid Interface Sci.*, **26**, 62 (1968).
6. Shubin V.A., Kim W., Safonov V.P., Sarychev A.K., Armstrong R.L., Shalaev V.M. *J. Lightwave Technol.*, **17**, 2183 (1999).
7. Joannopoulos J.D., Meade R., Winn J. *Photonic Crystals, Molding the Glow of Light* (Princeton, NJ: Princeton University Press, 1995).
8. Shkunov M.N., DeLong M.C., Raikh M.E., Vardeny Z.V., Zakhidov A.A., Baughman R.P. *Synthetic Metals*, **116**, 485 (2001).
9. Letokhov V.S. *Zh. Eksp. Teor. Fiz.*, **53** (4), 1442 (1967).
10. Markushev V., Zolin I., Briskina S. *Kvantovaya Elektron.*, **13**, 427 (1986) [*Sov. J. Quantum Electron.*, **16**, 281 (1986)].
11. Van Albada M.P., Lagendijk A. *Phys. Rev. Lett.*, **55**, 2692 (1985).
12. Frolov S.V., Vardeny Z.V., Zakhidov A.A., Baughman R.P. *Opt. Commun.*, **162**, 241 (1999).
13. Shkunov M.N., Vardeny Z.V., DeLong M.C., Polson R.C., Zakhidov A.A., Baughman R.P. *Advan. Funct. Mater.*, **12**, 21 (2002).